# Synthesis and Characterization of New Polyurea Elastomers by Sol/Gel Chemistry[a]

Antoni Sánchez-Ferrer,* Daniel Rogez, Philippe Martinoty

A series of elastomers based on polyurea chemistry is synthesized by crosslinking amino-terminated polyethers with a triisocyanate using an appropriate solvent, which slowed down the reactivity of the amino groups. Control of the reactivity allows the shaping of the material, and films of defined thickness can be achieved for mechanical testing. The strength of the final network can be tuned by the crosslinking density of the network chemical constitution. The resulting materials show a good thermal stability and promising mechanical enhancement.

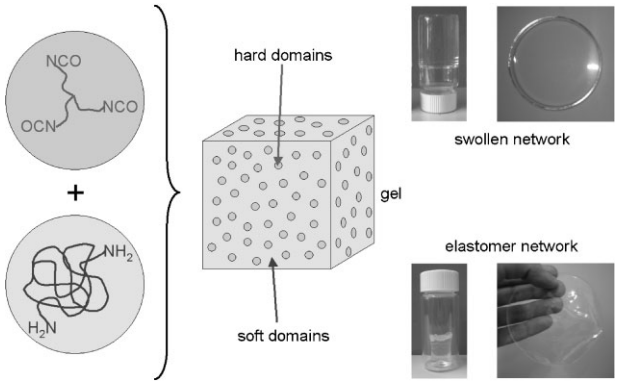


## Introduction

Polyurea chemistry is a relatively new synthetic process, similar to the one used for the synthesis of polyurethanes. But unlike the polyurethanes, polyureas do not require a catalyst to accelerate the chemical reaction, due to the high nucleophilicity of amines.[1] The relative reactivity of isocyanates with primary amines to form polyureas is 1 000 times faster than that of alcohols to form polyurethanes, or water to hydrolyze isocyanates, and thus foaming is almost impossible. This fast reactivity leads to the fact that curing of polyureas is not affected by moisture or temperature.[2]

Polyurea systems are the result of a chemical reaction between a polyisocyanate and a polyamine to form urea groups that can interact by hydrogen bonding. These systems have better resistance to high pH, far superior thermal properties and much higher melting points than hybrids, polyurethane systems or other polymers.[3–9] The urea linkage found in polyureas is more resistant to hydrolysis than the urethane linkage because of its bidentate nature.[10] The greatest advantages of polyureas are extreme resistance to abrasion and chemicals, and also service temperatures from −60 to +200 °C. Polyurethanes and polyurea block copolymers have acceptance in biomedical applications, as implants or medical devices,[11,12] due to their good biocompatibility and their excellent physical properties.[13,14]

Generally, the reaction for obtaining linear polymers (thermoplastic block copolymers) takes place between a diisocyanate (aromatic or aliphatic) with an amino-terminated prepolymer or resin (generally aliphatic).[8,10,14–23]

Dr. A. Sánchez-Ferrer
Food and Soft Materials Science, Institute of Food, Nutrition and Health, ETH Zurich,
Schmelzbergstrasse 9, 8092 Zurich, Switzerland
Fax: +41 44 632 1603.; E-mail: antoni.sanchez@agrl.ethz.ch
Dr. A. Sánchez-Ferrer
Institute of Supramolecular Science and Engineering, University Louis Pasteur, 8 allée
Gaspard Monge, 67083 Strasbourg, France
E-mail: a.sanchez-ferrer@isis.u-strasbg.fr
Dr. D. Rogez, Dr. P. Martinoty
Institute Charles Sadron, UPR 22 CNRS, 23 rue du Loess, 67034 Strasbourg Cedex, France

[a] Supporting information for this article is available at the bottom of the article's abstract page, which can be accessed from the journal's homepage at http://www.mcp-journal.de, or from the author.


*Macromol. Chem. Phys.* **2010**, *211*, 1712–1721

DOI: 10.1002/macp.201000117

The prepolymer or resins contains both soft segments with low glass transition temperatures and amorphous melts, and hard domains with high glass transition and high melting temperatures due to hydrogen bonding[24,25] as physical crosslinks. Little work has been done for the synthesis and study of polymer networks because of the fast reactivity during chemical crosslinking, except by using spray or reaction injection molding. Because of this fast reaction, polyureas can be used in sprayable systems for coatings.[26] The spray technology was not developed until the 1990s,[27,28] following the reaction injection molding technique.[29–31]

In both techniques, the two components are processed using specialized industrial equipment at high pressure and mixed either i) directly prior to surface coating, or, ii) in a mold cavity to obtain coatings, membranes or various different shapes. Elastomeric systems based on polyurea chemistry have been formulated to produce high performance, rapid curing coatings and caulks.[32] Because of their fast gelation[1] (typically 2 to 3 s gelation time) and curing process (dry time of less than 10 s), polyureas can be applied in adverse warm and humid conditions that would normally inhibit the use of conventional chemistries like polyurethanes.

The most common chemicals used are aromatic isocyanates [4,4′-dicyclohexylmethane diisocyanate (HMDI), 1,4-diphenylmethane diisocyanate (MDI), toluene diisocyanate (TDI), or *p*-phenylene diisocyanate (*p*PDI)] and aliphatic isocyanates [1,6-hexane diisocyanate (HDI) or isophorone diisocyanate (IPDI)] together with diamino-terminated prepolymers, such as polyesters (polycaprolactone), polyethers [poly(ethylene oxide), poly(propylene oxide), or poly(tetramethylene oxide)], polycarbonates (hexamethylene polycarbonate), and polydimethylsiloxanes, which lead to aromatic polyureas that are sensitive to light and atmospheric degradation and are also difficult to be dissolved and processed.[29,33–34]

In this paper, the synthesis of a new kind of polyurea elastomer by sol-gel chemistry is presented, where the reactivity of the amino-terminated polymers is reduced by the capping of the amines by reaction with ketones. This process allows control of the gelation time from seconds to minutes or hours. Upon drying the gel, an elastomeric film of well-defined thickness is obtained by controlling the concentrations of the polymer and crosslinker, the volume of the reacting mixture and the area of the mold. The post-drying formation of hydrogen bonds between the urea motifs, as well as their effect on the elastomeric systems, is analyzed in terms of chemical composition of the studied samples. These systematic changes allow the observation of the mechanical behavior of networks with physical and chemical crosslinks as a function of the segmental molecular weights and the nature of the crosslinkers.

## Experimental Part

### Materials

The three linear diamino-terminated polyetheramines AD-400, AD-2000 and AD-4000 (Jeffamine® D-400, $\overline{M}_n = 400$ Da; Jeffamine® D-2000, $\overline{M}_n = 2\ 000$ Da; Jeffamine® D-4000, $\overline{M}_n = 4\ 000$ Da), the three star-like triamino-terminated polyetheramines AT-403, AT-3000 and AT-5000 (Jeffamine® T-403, $\overline{M}_n = 440$ Da; Jeffamine® T-3000, $\overline{M}_n = 3\ 000$ Da; Jeffamine® T-5000, $\overline{M}_n = 5\ 000$ Da) were supplied by Huntsman International LLC. The triisocyanate crosslinker BHI-100 (Basonat® HI-100, $\overline{M}_n = 505$ Da) was provided by BASF SE. All chemicals were used as received. Acetone and butan-2-one (Aldrich) were used without further purification for the crosslinking of the polyetheramines.

### Characterization Techniques

$^1$H NMR, $^{13}$C NMR, $^1$H-$^1$H homocorrelation and $^1$H-$^{13}$C heterocorrelation experiments were carried out at room temperature on a Bruker DPX-360 spectrometer operating at 360 and 90 MHz, respectively, for each spin, and using $CDCl_3$ or acetone-$d_6$ as solvents and as the internal standards.

$^1$H high-resolution magic-angle spinning (HR-MAS) NMR measurements were carried out on the swollen samples at room temperature – before and after thermal treatment at 200 °C for 24 h in an oven – on a Bruker Avance DSX-500 spectrometer operating at 500 MHz and using $CDCl_3$ as solvent.

Differential scanning calorimetry (DSC) experiments were carried out on a Netzsch DSC 200F3 Maia apparatus with heating- and cooling-rates of 5, 10 and 20 $K \cdot min^{-1}$ under nitrogen atmosphere, using 20 μL aluminum pans with holes. The first heating run was use to remove all effects due to thermal history of the sample and only second, third and fourth heating and cooling runs were used at different rates on the same piece of sample.

Fourier-transform infrared (FTIR) spectra of solid samples were recorded at room temperature with a Bruker Tensor 27 FTIR spectrometer and using a MKII golden gate single attenuated total reflection (ATR) system.

Thermal gravimetric analysis (TGA) experiments were performed using a TGA/SDTA851e apparatus from Mettler Toledo equipped with an autosampler TS0801R0, and 70 μL aluminum oxide crucibles. Measurements were performed at a temperature rate of 5 $K \cdot min^{-1}$ from 25 up to 600 °C with an air flow of 300 $mL \cdot min^{-1}$.

Swelling experiments were performed in pure acetone, water and mixtures of acetone/water at 25 °C for 24 h, to obtain information on the effective crosslinking density as compared to other elastomers. The sizes of the dry and swollen elastomer sample were determined using a Will Strübin-Wetzlar optical microscope, and their respective weight by using a Mettler Toledo AT250 analytical balance. The volumetric swelling parameter ($Q_x = \alpha_x^3$) is the ratio of the volume of the swollen to dry elastomer, where $\alpha_x$ is the volumetric linear swelling parameter. The mass-uptaking swelling parameter ($Q_m = \alpha_m^3$) is the ratio of the mass of the swollen to dry elastomer, where $\alpha_m$ is the mass-uptaking linear swelling parameter.

Stress/strain measurements were performed with a self-constructed apparatus. In a cell controlled by a Haake-F6

thermostat and equipped with a Pt100 thermoresistor, the sample was stretched by one Owis SM400 microstep motor and controlled by an Owis SMK01 microstep controller. The stress was measured by a HBM PW4FC3 transducer load cell (300 g) and analyzed by an HBM KW3073 high-performance strain gage indicator. All relevant data such as temperature, uniaxial strain ratio ($\lambda = L/L_0$, where $L$ and $L_0$ are the lengths of the film in the stretched and unstretched states) and uniaxial stress ($\sigma$) were continuously logged. A personal computer controlled the deformation stepwise as specified by a script file. After each deformation step, the uniaxial stress was recorded at equilibrium (determined by the slope and the standard deviation of the continuously logged data).

Simultaneous small- and wide-angle X-ray scattering (SAXS and WAXS) experiments were performed using a Philips PW 1730 rotating anode (4 kW) in order to obtain direct information on the SAXS and WAXS reflections. Cu K$\alpha$ radiation ($\lambda = 1.5418$ Å) filtered by a graphite monochromator and collimated by a 0.8 mm collimator was used. The incident beam was normal to the surface of the film. The scattered X-ray intensity was detected by a Schneider image plate system (700 × 700 pixels, 250 μm resolution). Samples were placed in a self-constructed holder where temperature was controlled by a Haake-F3 thermostat. An effective scattering-vector range of $0.2\ \text{nm}^{-1} < q < 30\ \text{nm}^{-1}$ is obtained, where $q$ is the scattering wave-vector defined as $q = 4\pi \sin(\theta)/\lambda$, with a scattering angle of $2\theta$.

### Preparation of Gels and Films

The capping process of the amines was done following the same procedure as the preparation of gels and films but using acetone-$d_6$, and registering the $^1$H NMR spectra every 0.5 h, when the full capping of the amines was observed after 1.5 h of mixing.

The typical procedure to obtain networks with 15% (w/v) of solid content is described next, giving as an example the synthesis of the elastomer ED-2000. In two separate 30 mL flasks, the polyetheramine (3.850 g in 8.78 g of acetone) and the crosslinker (0.651 g in 11.41 g of acetone) were dissolved. After 2 h with occasional shaking of the solutions, the contents of the two flasks were mixed and ready to put in a glass capsule. The cast sample was ambient dried after 24 h of reaction at room temperature to make sure a good crosslinking process took place.

## Results and Discussion

### Synthesis of Polyetherurea Elastomers

As mentioned in the introduction, amines are much more reactive than alcohols in the presence of isocyanates, and the aim of this work was to achieve a slowed reactivity of the amino groups by capping them, with the ultimate purpose of obtaining pure polyurea elastomers by the sol/gel chemistry procedure. It is well known that amines can condensate with ketones and aldehydes to form imines – ketimines or aldimines (Scheme 1). Since aldehydes are quite toxic and difficult to handle, acetone and butan-2-one were chosen to carry out the capping process for their availability, low toxicity and easy evaporation. Solutions of the polyetheramines in acetone (alternatively, also butan-2-one) reduced drastically the reactivity of the amino polymers when reacting with isocyanates.

$^1$H NMR and $^{13}$C NMR spectra were measured on the solution of these amino compounds in a non-capping solvent ($CDCl_3$), and in a ketone (acetone-$d_6$). The results are shown in Figure 1. The formation of the imine can be monitored from the $^1$H NMR spectrum, as well as from the corresponding $^{13}$C NMR spectrum. The chemical shift of the two methyl groups neighboring both terminal amines in $CDCl_3$ is $\delta(CH_3CHNH_2) = 0.97$ (d, $J = 6.2$ Hz), while in acetone-$d_6$ it is $\delta(CH_3CHNH_2) = 0.95$ (d, $J = 6.4$ Hz). After the formation of the imine, these two methyl groups have a chemical shift of $\delta(CH_3CHNH_2) = 0.99$ (d, $J = 6.3$ Hz). The two protons neighboring the methyl group and in the $\alpha$-position to the amine have a chemical shift in $CDCl_3$ of $\delta(CH_3CHNH_2) = 2.96$–$3.08$ (m), but in acetone-$d_6$ this is

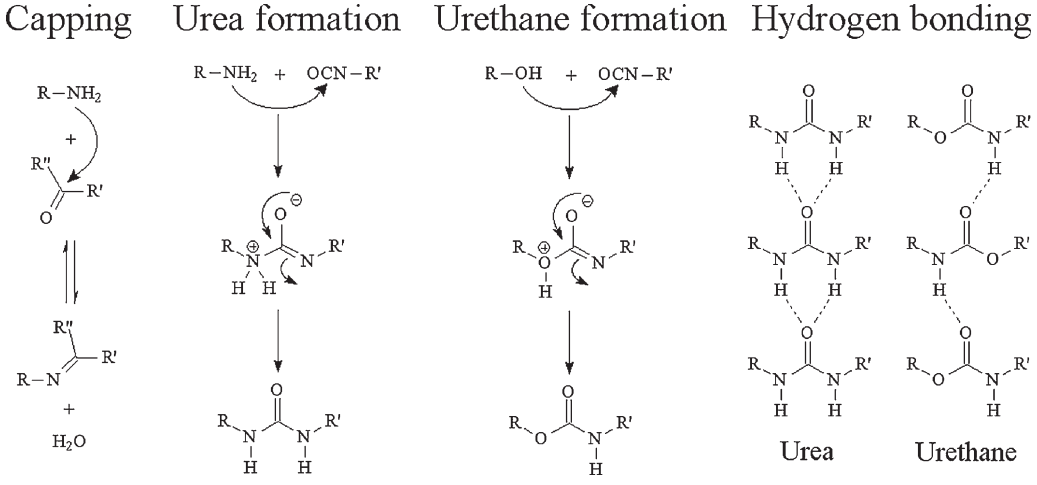


*Scheme 1.* Chemical representation of the capping process of amines with ketones or aldehydes, formation of urea or urethane linkage, and hydrogen bonding between urea (bidentate) and urethane (monodentate) motifs.


*Macromol. Chem. Phys.* **2010**, *211*, 1712–1721

Macromolecular Journals
DOI: 10.1002/macp.201000117

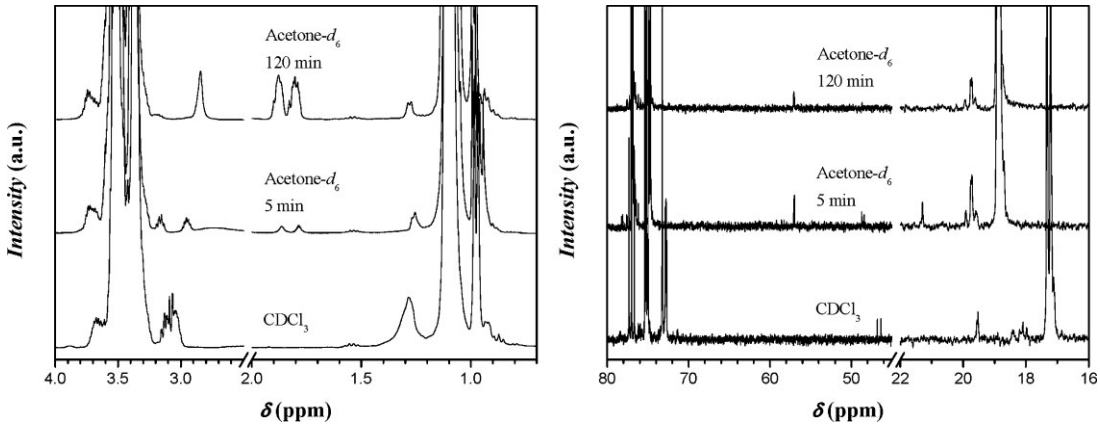


*Figure 1.* $^1$H and $^{13}$C NMR spectra of the amine AD-2000 in $CDCl_3$ and acetone-$d_6$ (5 and 120 min after solution preparation).

$\delta(CH_3CHNH_2) = 2.90–3.05$ (m). The same protons following imine formation have a new chemical shift of $\delta(CH_3CHN=C) = 3.56–3.66$ (m). One interesting sign of the formation of the imines is the appearance of two multiplets (almost quintuplets) in acetone-$d_6$ at $\delta = 1.75–1.84$ and 1.84–1.93 that correspond to one proton in *cis* or *trans* position to the condensed acetone with the amine. All these results were confirmed by $^1$H-$^1$H homocorrelation and $^1$H-$^{13}$C heterocorrelation experiments. The two carbon atoms in the $\alpha$-position to the nitrogen show a clearly different chemical shift in $CDCl_3$ of $\delta(CHNH_2) = 46.3$ and 46.8, with respect to in acetone-$d_6$: $\delta(CHNH_2) = 48.4$ and 48.7. The formation of the imine compound is detected by the presence in acetone-$d_6$ of two peaks at $\delta(CHN=C) = 57.0$ and 57.1. To conclude, the carbon corresponding to the condensed acetone to the amine appears as a broad peak at $\delta(C_2D_6\ C=N) = 166.0$ (see the Supporting Information).

After the optimization of the capping process of the amines in acetone, a final 15% (w/v) of solid content was chosen to prevent both precipitation among higher concentrations and incomplete crosslinking in more dilute systems. Commonly, amines ($-NH_2$) react in the presence of isocyanates ($-NCO$) resulting in the formation of a urea linkage, in the same manner that alcohols ($-OH$) form a urethane linkage (Scheme 1). Thus, since polymers with amino-terminated functionalities are present and the final repeating unit is a urea, the term polyurea then applies, as polyurethane applies in the case of hydroxyl-terminated polymers.

For the polyetherdiamines AD-400, AD-2000 and AD-4000, the corresponding polyurea elastomers ED-400, ED-2000 and ED-4000 contain only crosslinking points that come from the triisocyanate crosslinker. Similarly, the polyethertriamines AT-403, AT-3000 and AT-5000 led to the corresponding polyurea elastomers ET-403, ET-3000 and ET-5000 with two different crosslinkings: one from the triisocyanate and the other already present glycerol unit in the polyethertriamines (Scheme 2).

## Hydrogen Bonding in Polyetherurea Elastomers

It was expected that the polyureas would be mechanically stronger than the corresponding polyurethanes. The main reason is the presence of higher number of hydrogen bonds between the urea motifs and the localization of up to two per carbonyl group between two urea units (Scheme 1). Polyurethanes have fewer chances to build hydrogen bonds and they are not well-localized, and allow more freedom during the linkage of the carbamates.[35]

As mentioned above, in polyurea elastomers intermolecular hydrogen bonds are formed between the active hydrogen atoms of one urea donor group ($-NH-$) and the acceptor carbonyl group from another urea motif ($-CO-$). The formation of hydrogen bonds with other carbonyl-type groups like esters, amides and carbamates, and rarely with alcohols or ethers, is also possible. Infrared investigations of N–H stretching-related adsorptions showed that more than 90% of the $-NH-$ from urea or from urethane forms hydrogen bonds, representing a larger content than other functionalities.[18] Other studies showed that the formation of hydrogen bonds depends on the size of the segments at both sides of the urea linkage.[17] In polymers with high urea concentration, hydrogen bonds between $-NH-$ and $-CO-$ groups are more frequent. When the urea concentration is reduced, connections between $-NH-$ and $-CO-$ groups become less effective.

IR spectroscopic analyses of all the initial polyetheramines and their corresponding elastomers were performed in order to establish possible differences and predict the mechanical properties of the networks (Figure 2). The isocyanate crosslinker has some specific adsorption bands that correspond to the methylene groups ($CH_2\ \gamma$ 767 cm$^{-1}$; $CH_2\ \delta$, 1 456 cm$^{-1}$), the isocyanates (N=C=O st sym, 1 374–1 336 cm$^{-1}$; N = C = O st as, 2 258 cm$^{-1}$), and the isocyanurate ring ($[NCO]_3$, 1 679 cm$^{-1}$). The polyetheramines have some specific adsorption bands from the ether groups ($CH-O-CH_2$ st sym, 926 cm$^{-1}$; $CH-O-CH_2$ st as, 1

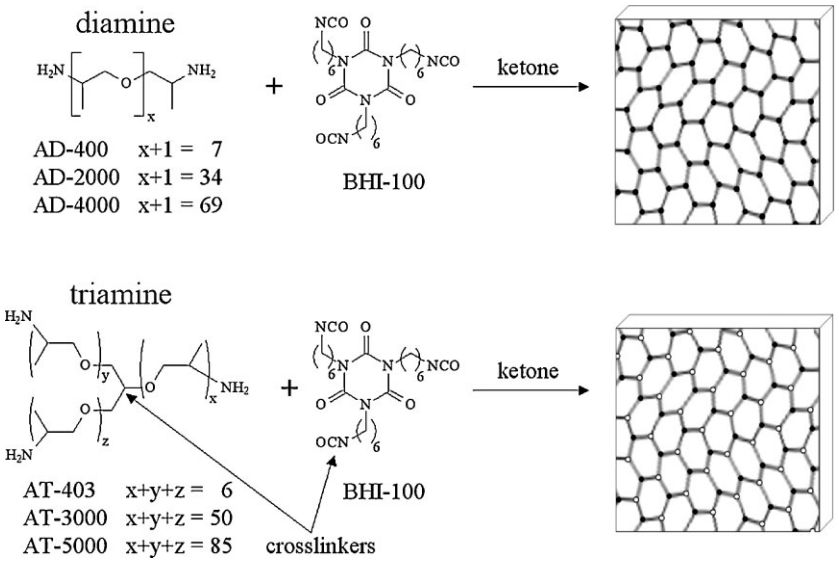


*Scheme 2.* Chemical structures of the polyetheramines (diamines and triamines), the triisocyanate crosslinker, and sketch of the corresponding networks (black dots are the BHI-100 crosslinkers; white dots are the glycerol crosslinkers).

096 $cm^{-1}$) and the amines (C–N st, 1 013 $cm^{-1}$). All polyetherurea elastomers show these peaks except for those coming from the isocyanates. A new peak appears as an indication of urea linkage formation, where one urea carbonyl is bonded to two NH groups, forming a bidentate hydrogen bonding (C=O amide I, 1 627 $cm^{-1}$). Other indications of hydrogen bonding and urea formation are the peaks at 1 569 $cm^{-1}$ (CO–N–H amide II) and at 3 334 $cm^{-1}$ (N–H st, hydrogen bonded). The peak at $\tilde{\nu} = 1$ 688 $cm^{-1}$ corresponds to the isocyanurate ring $[NCO]_3$ originally from the crosslinker, which has the same intensity as the methylene bending vibration. With this chemical architecture, where the hard domains containing the hydrogen bonding are well-localized, no presence of free urea ($\tilde{\nu} = 1\ 687\ cm^{-1}$) or monodentate hydrogen bonding ($\tilde{\nu} = 1\ 662\ cm^{-1}$) was observed[25] (see the Supporting Information).

The intensity of the IR peaks corresponding to the urea formation and hydrogen bonding, as well as those coming from the crosslinker, decreases with increasing molecular weight of the polyetheramine, since the crosslinking density is decreasing and fewer urea units are formed in the elastomeric sample. Even by decreasing the crosslinking density, the ratio between the hydrogen bonding and the urea peak is kept almost constant for all samples – which is an indication of good hydrogen bonding even at high segmental molecular weight.

SAXS and WAXS experiments were performed for the observation of any structural evidence of segment segregation between the poly(propylene) oxide block from the polyetheramines and the polyethylene block from the crosslinker (Figure 3). At low $q$ values, all samples show a broad peak around $0.85\ nm^{-1} < q < 1.85\ nm^{-1}$, which corresponds to the phase separation of the hydrogen bonding hard domains from the soft polyether domains.[36] The broadness of the peaks can be explain by the immobilization of these hard domains during the sol-gel process, the polydispersity of the polyetheramines and defects during drying. For samples with high volume fractions of the crosslinker (ED-400, $\phi_X = 0.39$; ET403, $\phi_X = 0.47$), the weak peak appears at $q$ values of 1.42 $nm^{-1}$ (44 Å) and 1.85 $nm^{-1}$ (34 Å), respectively. The rest of samples with lower volume fractions of the triisocyanate (ED-2000, $\phi_X = 0.12$; ED-4000, $\phi_X = 0.07$; ET3000, $\phi_X = 0.12$; ET5000, $\phi_X = 0.07$) have their corresponding strong peak at $q$ values of 0.98 (64 Å), 0.86 (73 Å), 0.92 (68 Å) and 0.87 (72 Å) $nm^{-1}$. This peak is related to the microphase separation between the hard segments containing the urea motifs and the crosslinked polymer melts from the poly(propylene) oxide chains. The solubility parameter of the six methylene

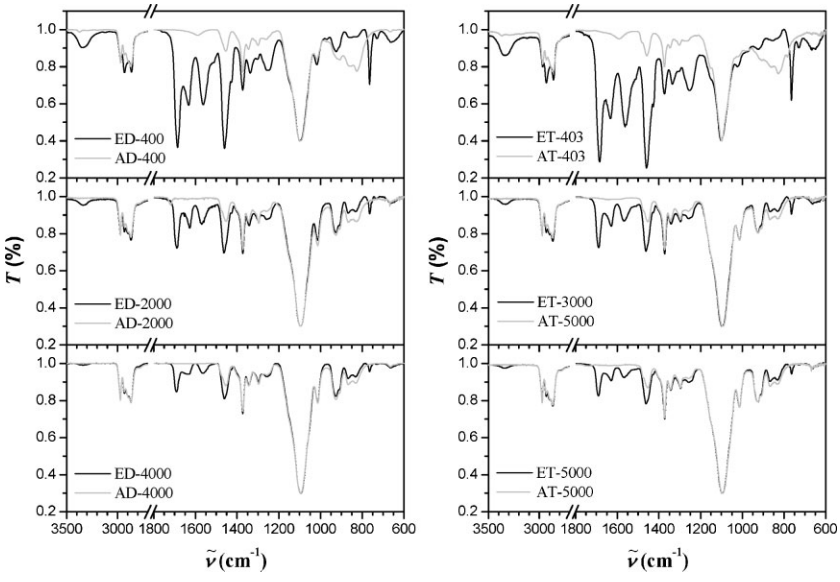


*Figure 2.* ATR-IR spectra of all amino-terminated polymers and their corresponding elastomers.


*Macromol. Chem. Phys.* **2010**, *211*, 1712–1721

DOI: 10.1002/macp.201000117

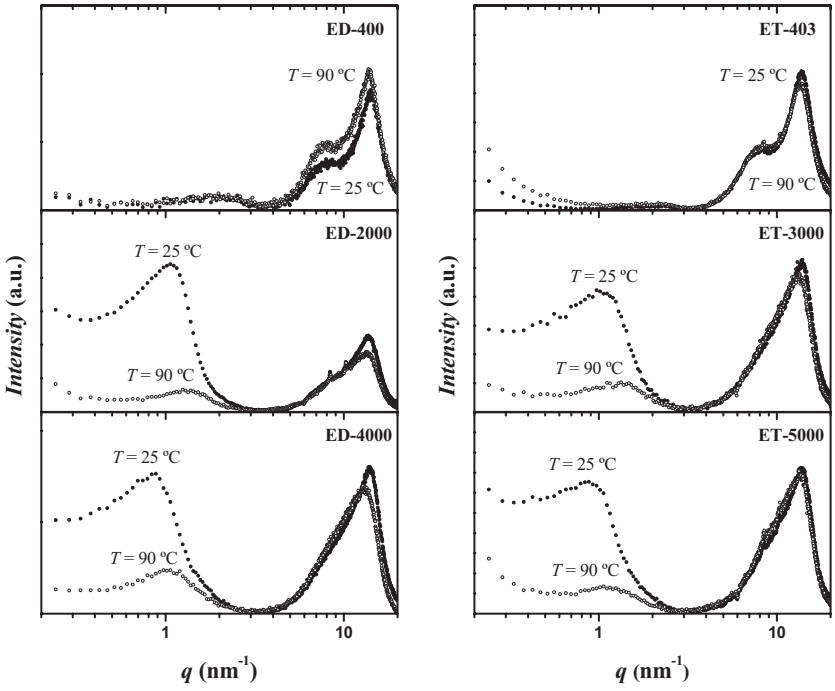


*Figure 3.* SAXS and WAXS curves of all elastomers at 25 °C (filled symbols) and 90 °C (empty symbols).

carbons from the crosslinker ($\delta = 16.2\ MPa^{1/2}$) is not that different from the corresponding solubility parameter of the poly(propylene oxide) chains ($\delta = 17.2\ MPa^{1/2}$),[37] which are soluble in acetone ($\delta = 19.7\ MPa^{1/2}$). However, as soon as the urea linkage is formed the solubility of the hard segment becomes too different to keep both segments together ($\delta = 45.6\ MPa^{1/2}$).[38–40] This might explain why all samples – even those having different volume fractions of the crosslinker – do show the same scattering pattern due to the localization of the hard segments in the crosslinking points. In Table 1, the comparison between the calculated full stretched segmental length ($l_c$) and the persistence length from the broad scattering peak calculated by SAXS ($d$) is presented, where one can observe that the latter are below the simulated value ($l_c$) expected in an isotropic polymer network.

At high $q$ values, two different distributions are observed; the first one, at $q = 7.7$ to $10.1\ nm^{-1}$ (8.1 or 6.3 Å), is related to the chain distance when two methyl groups from different propylene units see each other; the second one, at $q = 14.0\ nm^{-1}$ (4.5 Å), is the chain distance when no methyl steric hindrance is present and the polymer backbones interact with each other in the molten state. Surprisingly, for the highly crosslinked samples the first peak is shifted more to lower $q$ values with respect to the rest of the samples or the polymers themselves. The explanation lays in the fact that the short number of repeating units in the segments between crosslinking points, $DP_c$ (Table 1), forces the interaction between methyl groups located close in space, and a big steric effect appears and shifts the distance to higher values.

In order to check whether these networks have hydrogen bonding, X-ray experiments were also performed at higher temperature. In Figure 3, the experiments at 25 at 90 °C are shown, – a shift to higher $q$ values and a decrease in the intensity of the peaks at low $q$ values (SAXS) is observed, with changes in the relative intensity up to 80% of the initial value. This effect is reversible, and after cooling the samples the intensity of the peak increases as a sign of the restored hydrogen bonds.

## Thermal Properties of Polyetherurea Elastomers

Aliphatic polyurea systems have a low glass transition temperature, $T_g$, lower than the aromatic polyurea systems,

*Table 1.* Number-average molecular weight ($\overline{M}_n$) of the polyetheramines; segmental degree of polymerization ($DP_c$), segmental molecular weight ($\overline{M}_c$), segmental length ($l_c$), persistence length ($d$), volume fraction of the crosslinker ($\phi_x$), crosslinking density ($CD$), and density ($\rho$) of all polyetherurea elastomers.

| Sample | $\overline{M}_n$ | $DP_c$ | $\overline{M}_c$ | $l_c$ | $d$ | $\phi_x$ | $CD$ | $\rho$ |
|---|---|---|---|---|---|---|---|---|
| | $g \cdot mol^{-1}$ | | $g \cdot mol^{-1}$ | Å | Å | v/v | mol-% | $g \cdot mL^{-1}$ |
| ED-400 | 428 | 13 | 691 | 52 | 44 | 0.39 | 8.7 | 1.05 |
| ED-2000 | 1 991 | 40 | 2 259 | 149 | 64 | 0.12 | 1.9 | 1.01 |
| ED-4000 | 4 024 | 75 | 4 292 | 274 | 73 | 0.07 | 1.0 | 1.01 |
| ET-403 | 480 | 5 | 258 | 20 | 34 | 0.47 | 25.0 | 1.07 |
| ET-3000 | 3 007 | 20 | 1 110 | 74 | 68 | 0.12 | 3.8 | 1.02 |
| ET-5000 | 5 040 | 31 | 1 788 | 114 | 72 | 0.07 | 2.3 | 1.01 |

while also possessing an excellent resistance to degradation by UV light and color stability, and, unlike aromatic systems, are not subject to chemical oxidation.[41] DSC, TGA and HR-MAS NMR experiments were performed in order to check the stability of these aliphatic polymer networks and their thermal behavior.

DSC experiments already show some notable differences between the polyetheramines and their corresponding networks (Figure 4). The glass transition temperature of the elastomers is a bit higher and broader than their original polymers due to the crosslinking effect. The polymer networks show a broad endothermic peak (not present in the highly crosslinked networks ED-400 and ET-403) from 30 to 80 °C and with a low latent heat of $\Delta H = 4$ to 7 J · g$^{-1}$ in the range of low interactions like in liquid-crystals and hydrogen bonds. No order-to-disorder transition temperature or melting temperature of the hard segments were observed, because these hard segments are localized at the crosslinking points and are not free to move and rearrange themselves.

The thermal stability was checked by thermogravimetric analysis, where the degradation of the sample can be monitored. In Figure 5, the thermograms of one elastomeric sample (ED-2000) are shown where temperatures of more than 200 °C are needed to start the decomposition and degradation of the network. Samples with high crosslinker concentration are more suitable to degradation due to the high content of isocyanurate rings, which can undergo to other structures, rearrangements or decompose. In Table 2, all the thermal properties of the six elastomeric samples are shown.

Finally, in order to prove the chemical stability of the networks, all samples were analyzed by $^1$H HR-MAS NMR spectroscopy in the swollen state before and after thermal treatment. All samples were heated in an oven at 200 °C for 24 h at atmospheric pressure in order to observe any degradation. Results and aspect of the samples confirmed the high stability of the polyetherurea networks, as can be observed in Figure 6. Samples before and after heating in the presence of air did not show any differences in their chemical shifts.

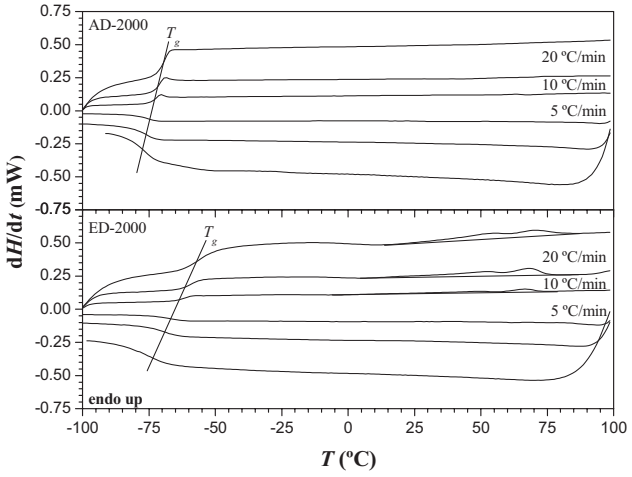


*Figure 4.* DSC thermograms of an amino-terminated polymer (AD-2000) and its corresponding polyurea network (ED-2000).

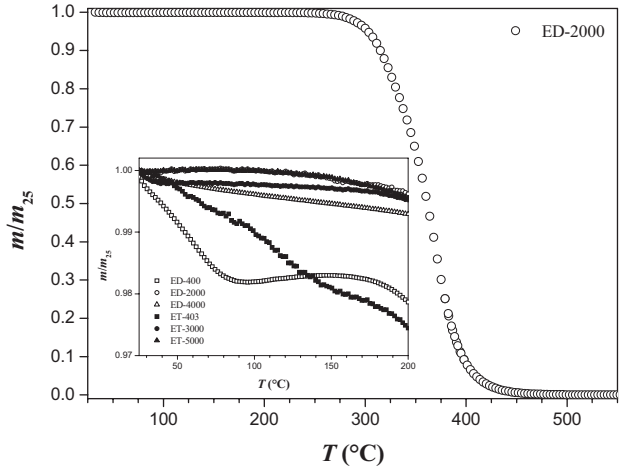


*Figure 5.* TGA thermograms of the polyurea network ED-2000 and for all samples to 200 °C (inset).

## Mechanical and Swelling Properties of Polyetherurea Elastomers

The degree of crosslinking is a parameter related to the mechanical properties and swelling of the networks, but in polyetherurea systems other factors might contribute, for example, the dimensions of the hard and soft domains, intermolecular hydrogen bonds, Van der Waals interactions, dipole-dipole interactions, π–π stacking aromatic interactions and others. The flexibility of the final elastomer will depend on the nature of the flexible segments with low glass transition, while the mechanical strength will be

*Table 2.* Thermal properties of the polyetherurea networks: glass transition temperature ($T_g$), heat capacity ($\Delta C_p$), hydrogen bonding breaking temperature ($T_H$), latent heat ($\Delta H$), and mass ratio at 200 °C ($m_{200}/m_{25}$).

| Sample | $T_g$ | $\Delta C_p$ | $T_H$ | $\Delta H$ | $m_{200}/m_{25}$ |
|---|---|---|---|---|---|
| | °C | J · g$^{-1}$ · K$^{-1}$ | °C | J · g$^{-1}$ | |
| ED-400 | −5 | 0.31 | – | – | 0.979 |
| ED-2000 | −65 | 0.50 | 63 | 5.4 | 0.996 |
| ED-4000 | −71 | 0.37 | 42 | 3.8 | 0.993 |
| ET-403 | +10 | 0.34 | – | – | 0.974 |
| ET-3000 | −60 | 0.52 | 42 | 7.2 | 0.995 |
| ET-5000 | −67 | 0.52 | 37 | 5.9 | 0.995 |


*Macromol. Chem. Phys.* **2010**, *211*, 1712–1721

Macromolecular Journals

DOI: 10.1002/macp.201000117

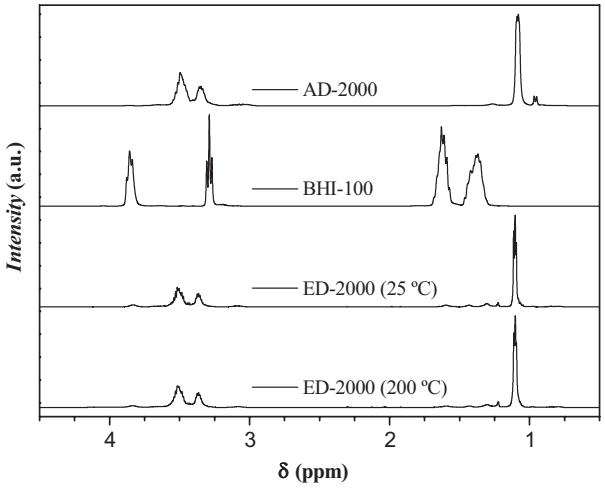


*Figure 6.* $^1$H NMR (HR-MAS) spectra of the amino-terminated polymer (AD-2000), the crosslinker (BHI-100) and the corresponding elastomer (ED-2000) at 25 °C and after 24 h at 200 °C.

given by the hard segments with high melting points (for thermoplastic block copolymers)[42] or the number of crosslinking points (for polymer networks).

One important parameter to be measured before any swelling or mechanical experiments is the analysis of the soluble content (*sc*) of the network. This quantity is related to small fragments that were not attached to the polymer matrix. The values obtained for the soluble content are listed in Table 3, where values below 10% indicate well-defined networks through crosslinking.

The swelling process is the result of the equilibrium between the two forces involved between the solvent molecules solvating the polymer chains of the network (mixing) and the retractive elastic force of those chains tending to keep their original conformation (elasticity). Thus, samples that show higher degrees of crosslinking should present lower degrees of swelling, and vice versa.

In Table 3, the linear swelling parameter ($\alpha_x = x/x_0$, where $x$ and $x_0$ are the dimensions of the elastomer after and before swelling) and the mass-uptaking linear swelling parameter ($\alpha_m = m_s^{1/3}/m_e^{1/3} \cdot \rho_e^{1/3}/\rho_s^{1/3}$, where $m_s$ and $\rho_s$ are the mass-uptaking and density of the solvent, and $m_e$ and $\rho_e$ the mass and density of the elastomer) are shown for all elastomers when swollen in acetone at 25 °C. For better visualization, in Figure 7a, the linear mass-uptaking swelling parameter ($\alpha_m$) is plotted as a function of the linear swelling parameter ($\alpha_x$), and the resulting fitted curve shows good agreement with both techniques when evaluating the swelling behavior of all networks. Thus, samples with higher degree of crosslinking or shorter segmental molecular weight (ET-403) swell less than those with lower crosslinker content or longer segmental molecular weight (ED-4000).

*Table 3.* Swelling parameters ($\alpha_x$ and $\alpha_m$), crosslinking density (*CD*) soluble content (*sc*), segmental molecular weights ($\overline{M}_c$), and Young's modulus (*E*).

| Sample | $\alpha_x$ | $\alpha_m$ | *CD* | *sc* | $\overline{M}_c$ | *E* |
|---|---|---|---|---|---|---|
| | | | mol-% | wt.-% | g · mol$^{-1}$ | MPa |
| ED-400 | 1.19 | 1.22 | 8.7 | 2.4 | 691 | 5.0 |
| ED-2000 | 1.87 | 1.94 | 1.9 | 5.8 | 2 259 | 0.8 |
| ED-4000 | 2.00 | 2.11 | 1.0 | 6.3 | 4 292 | 0.2 |
| ET-403 | 1.08 | 1.17 | 25.0 | 4.1 | 258 | 10.5 |
| ET-3000 | 1.69 | 1.71 | 3.8 | 2.2 | 1 110 | 2.3 |
| ET-5000 | 1.80 | 1.86 | 2.3 | 6.1 | 1 788 | 2.0 |

The estimation of the Flory-Huggins parameter ($\chi$) for poly(propylene oxide), polyethylene, and polyurea when mixed with acetone by using their Hildebrand solubility parameters ($\delta$) gave values of $\chi_{PPO} = 0.266$, $\chi_{PE} = 0.237$ and $\chi_{polyurea} = 1.106$, showing that the first two polymers are mixable with acetone but not the polyurea. By using the relation $\alpha_x = [\overline{M}_c\ (0.5 - \chi)/RT]^{1/5}$ (from Flory's swelling theory;[43–44] where $\alpha_x$ is the linear swelling parameter and $\overline{M}_c$ is the segmental molecular weight) (Table 3), the Flory-Huggins parameter for the obtained elastomers is estimated as $\chi = 0.323$. This value is a bit higher than the corresponding parameter of poly(propylene oxide), with the difference being due to the presence of urea motifs in the network.

The swelling of the networks strongly depends on the nature of the solvent.[45–46] Thus, for a good solvent the network will swell to a certain limit depending on the equilibrium of forces, but for a bad solvent no swelling is expected. Acetone was chosen as a good solvent ($\delta = 19.7$ MPa$^{1/2}$) and water as a bad one ($\delta = 48.0$ MPa$^{1/2}$) for the poly(propylene oxide) chains ($\delta = 17.2$ MPa$^{1/2}$). Mixtures of both solvents at different proportions were used in order to observe the degree of swelling at different solubilities. By decreasing the volume fraction of the good solvent all networks should swell less but still inversely proportional to the degree of crosslinking. In Figure 7b, the degree of swelling as function of the volume fraction of acetone is shown, where mixtures with less than 25% acetone no longer swell. These elastomers are useful as sealants against water.

Finally, the mechanical behavior of all elastomers was determined and correlated to the segmental molecular weight ($\overline{M}_c$) by performing stress/strain experiments. In the elastic region – for small deformations – the linear behavior between the true stress and the applied strain allows the calculation of Young's modulus (*E*). In Figure 8, the stress/strain curves are plotted. The data corresponds to the elastic moduli collected in Table 3. Young's modulus increases with increasing crosslinking density or decreasing number of repeating units between crosslinking

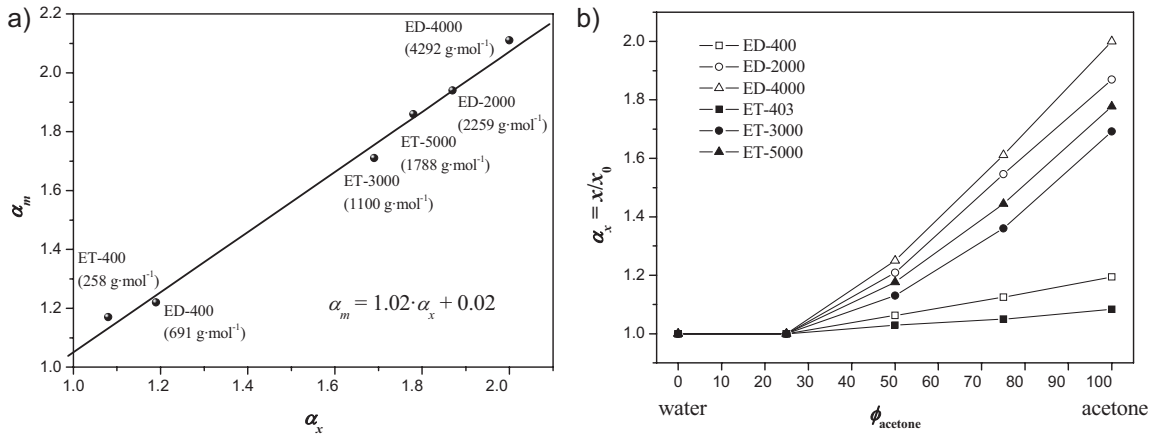


*Figure 7.* a) The linear swelling parameter ($\alpha_x$) versus the mass-uptaking linear swelling parameter ($\alpha_m$) for all samples with their corresponding segmental molecular weights, $\overline{M}_c$. b) Linear swelling parameter ($\alpha_x$) of all samples as function of the volume fraction of acetone ($\phi_{acetone}$) in mixtures of acetone/water at 25 °C.

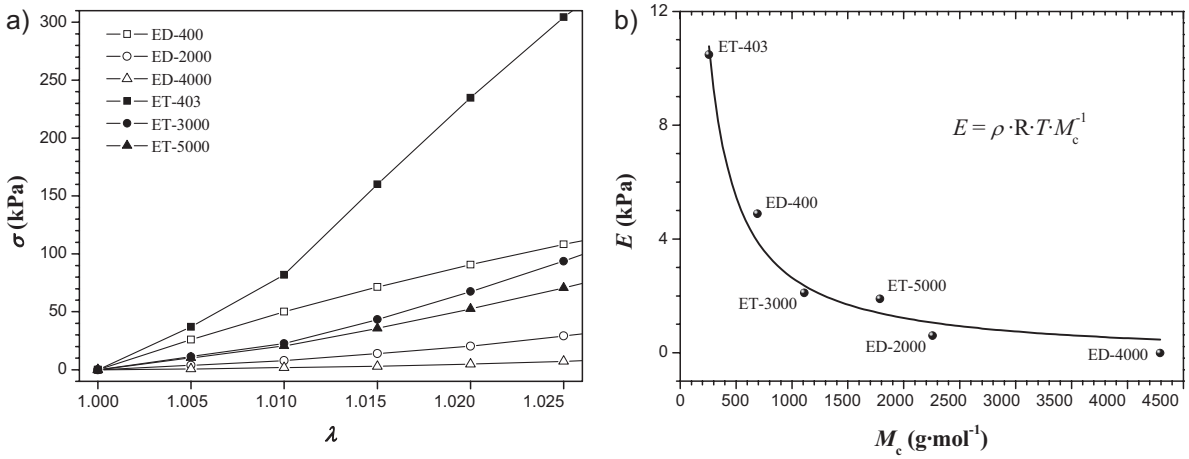


*Figure 8.* a) Stress/strain experiments on all the polyetherurea elastomers at 25 °C. b) Young's modulus ($E$) as function of the segmental molecular weight ($\overline{M}_c$).

points. In other words, the elastic modulus is inversely proportional to the segmental molecular weight of the network.

To sum up and determine this proportionality, Young's modulus was plotted against the segmental molecular weight (Figure 8b) by applying the equation $E = \rho RT/\overline{M}_c$,[47] using the classical rubber elasticity theory for ideal networks.[48] The result shows a reciprocal function, where the obtained average density of the network is $\rho = 1.13 \pm 0.09\ g \cdot mL^{-1}$, very close to the theoretical average density of $\rho = 1.03\ g \cdot mL^{-1}$. Further shear stress/strain experiments have been performed, and their results will be published soon, as well as the incorporation of magnetic nanoparticles for the synthesis of hybrid nanocomposites, which could work as a actuators or as a energy generators.[49]

## Conclusion

A new method has been developed to obtain polyurea elastomers by organic sol/gel chemistry. The key point of this process is the capping of amino-terminated polymers which slows down their reactivity when reacting with isocyanates. This slowed reactivity was proved by the formation of the imine compound, confirmed by several NMR techniques ($^1$H, $^{13}$C, $^1$H-$^1$H and $^1$H-$^{13}$C). The control in the synthesis of polyurea networks results in systems with good thermal stability, low soluble content and more easily tunable mechanical performance with respect to conventional polyurethane, polyurethane/polyurea networks, or thermoplastic block copolymers.

The localized urea crosslinkers in the hard segments and the architecture of the amino-terminated building block


*Macromol. Chem. Phys.* **2010**, *211*, 1712–1721

Macromolecular Journals
DOI: 10.1002/macp.201000117

play an important role in the elastomeric behavior, where physical (hydrogen bonding) and chemical (urea linkage) networks work together in one system. Only bidentate hydrogen bonding has been found by ATR-IR spectroscopy. The micro-phase separated domains were confirmed by SAXS, where embedded hard domains in a soft polymer matrix are present. The aliphatic polyurea networks show a good resistance to degradation and high transparency stability due to the absence of aromatic moieties. This stability was analyzed and confirmed by DSC, TGA and HR-MAS NMR experiments, showing a large operational temperature window from $-60$ up to $+200\,^{\circ}C$ or more. Finally, stress/strain and swelling experiments demonstrated the correlation between the crosslinking density and the mechanical properties of the samples, showing that lower swelling ratios and higher Young's moduli are observed with high crosslinked samples (low segmental molecular weight), and vice versa.

Acknowledgements: We are grateful to Prof. *Heino Finkelmann* (Institute for Macromolecular Chemistry, Freiburg, Germany) for allowing some measurements in his research group, Dr. *Laura Ramón-Giménez* and Dr. *Patrick Heinze* (Institute for Macromolecular Chemistry, Freiburg, Germany) for their support and help during some experiments, and *Huntsman International LLC* and *BASF SE* for kindly providing all the chemicals.

Received: March 4, 2010; Revised: April 6, 2010; Published online: June 30, 2010; DOI: 10.1002/macp.201000117

Keywords: crosslinking; elastomers; gels; polyurea; sol-gel

[1] D. M. Berger, D. J Primeaux, II, "Thick-Film Elastomeric Polyurethanes and Polyureas", in: *The Inspection of Coatings and Linings*, 2nd edition, The Society for Protective Coatings, Pittsburgh 2003, Chapter 5.3.
[2] W. D. Vilar, *Chemistry and Technology of Polyurethanes*, 2nd edition, Vilar Polyurethanes, Rio de Janeiro 2002.
[3] R. Hill, E. E. Walker, *J. Polym. Sci.* **1948**, *3*, 609.
[4] I. A. Mahammad, V. Mahadevan, M. Srinivasan, *Eur. Polym. J.* **1989**, *25*, 427.
[5] X. T. Tao, T. Watanabe, D. C. Zou, S. Shimoda, H. Sato, S. Miyata, *Macromolecules* **1995**, *28*, 2637.
[6] J. L. Stanford, R. H. Still, A. N. Wilkinson, *Polym. Int.* **1996**, *41*, 283.
[7] S. Wataru, C. Koki, T. Naoto, *J. Polym. Sci., Part B: Polym. Phys.* **2001**, *39*, 247.
[8] I. Yilgor, E. Yilgor, S. Das, G. L. Wilkes, *J. Polym. Sci., Part B: Polym. Phys.* **2009**, *47*, 471.
[9] S. K. Jewrajka, J. Kang, G. Erdodi, J. P. Kennedy, E. Yilgor, I. Yilgor, *J. Polym. Sci., Part A: Polym. Chem.* **2009**, *47*, 2787.
[10] S. Das, I. Yilgor, E. Yilgor, G. L. Wilkes, *Polymer* **2008**, *49*, 174.
[11] S. Braley, *J. Macromol. Sci.: Chem.* **1970**, *A4*, 529.
[12] P. K. Weathersby, T. Kolobow, E. W. Stool, *J. Biomed. Mater. Res.* **1975**, *9*, 561.
[13] J. H. Boretos, W. S. Pierce, *Science* **1967**, *158*, 1481.
[14] R. W. Hergenrother, X. H. Yut, S. L. Cooper, *Biomaterials* **1994**, *15*, 635.
[15] L. Ning, W. De-Ning, Y. Sheng-Kangt, *Polymer* **1996**, *37*, 3577.
[16] N. Samson, F. Mechin, J. P. Pascault, *J. Appl. Polym. Sci.* **1997**, *65*, 2265.
[17] S. Das, I. Yilgor, E. Yilgor, B. Inci, O. Tezgel, F. L. Beyer, G. L. Wilkes, *Polymer* **2007**, *48*, 290.
[18] J. Mattia, P. Painter, *Macromolecules* **2007**, *40*, 1546.
[19] X. L. Li, D. J. Chen, *J. Appl. Polym. Sci.* **2008**, *109*, 897.
[20] J. A. Pathak, J. N. Twigg, K. E. Nugent, D. L. Ho, E. K. Lin, P. H. Mott, C. G. Robertson, M. K. Vukmir, T. H. Epps, III, C. M. Roland, *Macromolecules* **2008**, *41*, 7543.
[21] J. B. Dai, H. C. Kuan, X. S. Du, S. C. Dai, J. Ma, *Polym. Int.* **2009**, *58*, 838.
[22] S. K. Jewrajka, E. Yilgor, I. Yilgor, J. P. Kennedy, *J. Polym. Sci., Part A: Polym. Chem.* **2009**, *47*, 38.
[23] D. Fragiadakis, R. Gamache, R. B. Bogoslovov, C. M. Roland, *Polymer* **2010**, *51*, 178.
[24] S. L. Cooper, A. V. Tobolsky, *J. Appl. Polym. Sci.* **1966**, *10*, 1837.
[25] M. M. Coleman, M. Sobkowiak, G. J. Pehlert, P. C. Painter, *Macromol. Chem. Phys.* **1997**, *198*, 117.
[26] R. L. Rowton, *J. Elastom. Plast.* **1977**, *9*, 365.
[27] M. Munstermann, T. Buchan, K. Von Diest, *Kunstst. Plast. Eur.* **2001**, *91*, 11.
[28] K. Buecking, *Eur. Coat. J.* **1998**, *10*, 730.
[29] W. R. Willkomm, Z. S. Chen, C. W. Macosko, D. A. Gobran, E. L. Thomas, *Polym. Eng. Sci.* **1988**, *28*, 888.
[30] J. L. Stanford, A. N. Wilkinson, D. K. Lee, A. J. Ryan, *Plast. Rubber Proc. Appl.* **1990**, *13*, 111.
[31] A. J. Ryan, J. L. Stanford, A. J. Birch, *Polymer* **1993**, *34*, 4874.
[32] D. J Primeaux, II, *J. Prot. Coat. Linings* **2001**, *18*, 26.
[33] A. J. Ryan, J. L. Stanford, A. N. Wilkinson, *Polym. Bull.* **1987**, *18*, 517.
[34] A. J. Ryan, *Polymer* **1990**, *31*, 707.
[35] B. D. Kaushiva, S. R. McCartney, G. R. Rossmy, G. L. Wilkes, *Polymer* **2000**, *41*, 285.
[36] G. L. Wilkes, S. Abouzahr, *Macromolecules* **1981**, *14*, 458.
[37] E. Morales, J. L. Acosta, *Polym. J.* **1996**, *28*, 127.
[38] D. W. van Krevelen, *Properties of Polymers*, Elsevier, Amsterdam 1992, Chapter 8.
[39] A. F. M. Barton, *Handbook of Polymer–Liquid Interaction Parameters and Solubility Parameters*, CRC Press, Englewood Cliffs, 1990.
[40] A. M. F. Barton, *Handbook of Solubility Parameters and Other Cohesiona Parameters*, 2nd edition, CRC Press, New York 1991.
[41] D. J Primeaux, II, *J. Elastom. Plast.* **1992**, *24*, 323.
[42] M. Furukawa, T. Shiiba, *Polymer* **1999**, *40*, 1791.
[43] B. Erman, B. M. Baysal, *Macromolecules* **1985**, *18*, 1696.
[44] N. A. Neuburger, B. E. Eichunger, *Macromolecules* **1988**, *21*, 3060.
[45] P. J. Flory, *J. Chem. Phys.* **1977**, *66*, 5720.
[46] P. J. Flory, *Principles of Polymer Chemistry*, Cornell University Press, New York 1983, Chapter XIII.
[47] J. Schätzle, W. Kaufhold, H. Finkelmann, *Makromol. Chem.* **1989**, *190*, 3269.
[48] R. A. Orwell, *Rubber Chem. Technol.* **1977**, *50*, 451.
[49] A. Sánchez-Ferrer, M. Reufer, R. Mezzenga, P. Schurtenberger, H. Dietsch, *Nanotechnology* **2010**, *21*, P 185603/1-7.